

---

# A DATA-DRIVEN DIAGNOSTIC FRAMEWORK FOR SMALL WATERSHEDS BASED ON MARKOV CHAIN-MONTE CARLO

---

A PREPRINT

 **Xiao Peng**

School of Civil and Environmental Engineering  
Cornell University  
Ithaca, NY 14850  
xp53@cornell.edu

 **John D. Albertson** \*

School of Civil and Environmental Engineering  
Cornell University  
Ithaca, NY 14850  
albertson@cornell.edu

August 27, 2021

## ABSTRACT

Understanding dynamics of hydrological properties is essential in producing skillful runoff forecast. This can be quantitatively done by tracking changes in parameters of hydrology models that represent physical characteristics. In this study, we implemented a Bayesian estimation method for small watersheds in continuously estimating hydrology model parameters given observations of precipitation and runoff. The method was coupled with a conceptual hydrology model of Instantaneous Unit Hydrograph model based on a modified Gamma distribution. The whole diagnostic framework was tested using simulated data as well as observational data from the Fall Creek watershed. Both analyses showed good consistency between Bayesian parameter estimations and true values or maximum likelihood estimations. Also for the case study using observational data, a systematic shift in local precipitation-runoff response was observed in 1943, which could not be learned by looking at times series of precipitation, runoff, and runoff coefficients. Our results demonstrated potential of the Bayesian estimation method in monitoring hydrological dynamics and rapidly detecting changes in hidden physical processes for small watersheds.

**Keywords** Precipitation-Runoff Response, Instantaneous Unit Hydrograph, Markov Chain-Monte Carlo, Bayesian Estimation

## 1 Introduction

Skillful runoff forecast is of great importance in informing decision making in water resource management across various sectors including but not limited to hydropower plant operation [Jiang et al., 2018], agriculture resource planning [Shah et al., 2017], and disaster mitigation [Pappenberger et al., 2005, Fundel et al., 2013]. Amplitudes of runoff at slow timescales (e.g. monthly to annual) are always largely monotonically determined by amplitudes of precipitation. However, some key variables for determining water-related disasters (e.g. flooding) like timing and amplitude of peak flow are decided by the precipitation-runoff response as controlled by local hydrological properties [Cunderlik and Ouarda, 2009, Do et al., 2020]. Though advances in monitoring technology are making massive data available at exceptionally fine resolutions [Ma et al., 2015], the observations are usually limited to easy-to-measure variables such as precipitation and runoff. It is hard to directly model dynamics in the local hydrological properties by looking at observations of these variables. For example, simply looking at amplitudes of precipitation and runoff (separately) will not offer any information on the temporal distribution of water.

It is well-established that some parameters of physically-based hydrology models are determined by physical characteristics of the watershed like river morphology [Hassan et al., 2006] or land use types [Heuvelmans et al., 2004]. Based on this fact, the problem of inferring underlying dynamics of precipitation-runoff response can then be refined to estimating the time-varying hidden variables (i.e. model parameter) given observations of some easy-to-measure

---

\*Corresponding author

variables (e.g. precipitation and runoff). Most methods designed for model calibration are suited for this job and they can be roughly categorized into two classes: 1) the Maximum Likelihood Estimation (MLE) method that searches for the optimal parameter values that maximize the likelihood function for a given set of observations [Sorooshian et al., 1983, Castiglioni et al., 2010]; and 2) the Bayesian method (also often referred to as the Maximum a Posteriori (MAP)) that estimates the probability distribution function (PDF) of parameters given observations [Bates and Campbell, 2001, Smith and Marshall, 2008]. Either approach has its own advantages and represents different perspectives of approaching a problem (MLE is often described as the frequentists' methodology while MAP is often described as the Bayesian's methodology [Nolan et al., 2021]). For situations where information of prior distributions and source of uncertainty is known, the Bayesian method is the preferable option since it can simultaneously estimate the optimal parameter values and quantify the associated uncertainty [Sivia and Skilling, 2006]. In addition, for high-dimensional problems, the simulated PDF usually converges to the true PDF at a controllable rate using Bayesian methods [Cowles and Carlin, 1996] while the computational cost can increase exponentially as number of parameter increases for MLE methods (e.g. grid search method) [Ba et al., 2017]. These advantages make the Bayesian model suitable for calibrating (or inferring) hydrology models since most of them use not multiple but many parameters [Devia et al., 2015].

In this paper, we propose to implement a diagnostic framework for monitoring changes in local hydrological properties by tracking estimations of hydrology model parameters given observations using a Bayesian estimation method. The framework is specifically designed for small watersheds. For large watersheds, a lot of information would be lost by aggregating spatially highly-heterogeneous hydrological properties into a few parameters and this would lead to huge uncertainty in parameter estimations. The model is tested using both simulated and observational data of precipitation and runoff, and the observational data was collected for the small watershed of Fall Creek at Ithaca NY.

## 2 Data

Fall Creek is a fourth-order stream that flows through Ithaca, NY and drains to Cayuga Lake. The watershed of Fall Creek has a relatively small drainage area of 324 km<sup>2</sup> and consists of mixed forested and agricultural areas [Knighton et al., 2017]. The precipitation-runoff response for most watershed in NY are found to be dominated by a saturation-excess process and runoff is usually only generated when and where soils are highly saturated [Easton et al., 2007, Dahlke et al., 2009]. The watershed is chosen for having relatively long records of ground-based precipitation and runoff observations at a daily timescale. Runoff data is collected from the National Water Information System (NWIS) of the United States Geological Survey (USGS) [U.S. Geological Survey, 1994]. The runoff station (USGS 04234000 Fall Creek) is located at [42°27'12"N, 76°28'22"W] and has a continuous record of runoff from February 1925 to current year. Precipitation data is collected from the Global Historical Climate Network-Daily (GHCN-D) database that integrates station-based observations from numerous sources in producing daily climate records with quality assurance [Durre et al., 2008, 2010, Menne et al., 2012]. The precipitation station (GHCND:USC00304174) is maintained by Cornell [42°26'57"N, 76°26'57"W] and has a continuous record of precipitation from April 1925 to current year. The study period is set to 1925-2017.

Since we want to focus on monitoring changes in local hydrological properties at a inter-annual scale in the case study, we removed the predominant effects of seasonality by only examining precipitation-runoff response during boreal summer (June-July-August). Instead of separating individual storm events before fitting the hydrology model, data over the whole summer is used to estimate optimal parameter values averaged for multiple storm events. And each summer period can be adaptively extended by moving the starting day earlier so that effects of prior storms events will not be missed. The summer period is extended if runoff at the starting day is higher than some thresholds (e.g. 90<sup>th</sup> percentile runoff value over the whole summer period) since this indicates non-negligible base flow resulted from prior storm events. A year is dropped if flow rate at the starting day is still large after extending the summer period for over 5 days. This step is guarantee consistency in lengths of summer periods and thus in comparing model performance across different periods since difference sample sizes can change absolute values of many performance metrics even at the same statistical significance level (e.g. the Pearson's correlation coefficient). Furthermore, summer periods with missing data are dropped. At last, 65 summer periods (70% of total 93 years) with lengths ranging in [92, 97] days are selected.

## 3 Methods

### 3.1 The Bayesian Estimation Scheme

Data pairs of precipitation  $P^t$  and runoff  $D^t$  at time  $t$  are denoted by  $D^t$  such that  $D^t = (P^t, R^t)$ . Assuming the local precipitation-runoff response is determined by some set of hidden parameters  $\Theta$  that not cannot be easily measured, the

goal of this study is to infer  $\Theta$  given some observations  $D$  (i.e. PDF of  $\Theta$  given  $D$ , or  $P(\Theta|D)$ ). Since it is hard to directly simulate  $P(\Theta|D)$ , the Bayes' Theorem is adopted as given by

$$P(\Theta|D) = \frac{P(D|\Theta) \cdot P(\Theta)}{P(D)} \quad (1)$$

The target PDF (often referred to as the posterior PDF)  $P(\Theta|D)$  can then be estimated by calculating the likelihood PDF  $P(D|\Theta)$ , the prior PDF  $P(\Theta)$ , and the evidence PDF  $P(D)$ . The evidence PDF  $P(D)$  can be regarded as a rescaling factor to make the resulting posterior PDF sum to one. Using the example of a continuous random variable  $\Theta$ ,  $P(D)$  can be solved by integrating over all possibilities of  $\Theta$  as given by

$$P(D) = \int P(D \cap \alpha) d\alpha = \int P(D|\alpha) \cdot P(\alpha) d\alpha \quad (2)$$

Analytical solutions for estimating the integral in Equation 2 are only available for some specific combinations of prior and likelihood functions (e.g. when they are both Gaussian (Kalman Filter)) [Welch et al., 1995, Eddy, 2004]. To numerically estimate the integral is always computationally intensive and even impossible for high dimensional random variables. Instead of directly solving the Equation 1, we propose to simulate the posterior PDF using a Markov Chain-Monte Carlo (MCMC) approach [Gilks et al., 1995], which avoid computing the evidence PDF. The classic Metropolis Hastings algorithm [Chib and Greenberg, 1995] is adopted here and consists of 3 major steps for constructing a Markov process of which the stationary distribution ( $\pi_\infty$ ) converges to the target posterior PDF.

1. Choose a transition kernel (also often referred to as a proposal distribution)  $q(y|x)$  such that  $q(y|x) > 0$  for all  $x, y \in \chi$  ( $\chi$  is the parameter space).
2. Define an acceptance rate  $\alpha_{x,y}$  as given by

$$\alpha_{x,y} = \frac{\pi_\infty(y)q(x|y)}{\pi_\infty(x)q(y|x)} \quad (3)$$

3. Repeatedly simulate the Markov process: at time  $k$ , given state  $x_k = x$ 
  - i) simulate next state of the Markov process  $y \sim q(y|x)$ ,
  - ii) generate  $u$  from an uniform distribution  $u \sim U[0, 1]$ ,
  - iii) if  $u < \alpha_{x,y}$ , set  $x_{k+1} = y$ ; otherwise, set  $x_{k+1} = x$ .

If we substitute the posterior PDF into Equation 3, the acceptance rate is given by

$$\alpha_{x,y} = \frac{P(y|D)q(x|y)}{P(x|D)q(y|x)} = \frac{P(D|y)P(y)q(x|y)}{P(D|x)P(x)q(y|x)} \quad (4)$$

The transition kernel essentially determines how fast the Markov process explores unknown parameter space. A variety of transition kernels have been developed and tested for improving efficiency of the MCMC algorithm [Yang and Rodríguez, 2013, Thawornwattana et al., 2018]. However, since intent of this study is to prove feasibility of Bayesian estimation in monitoring changes in hydrological response for small watersheds instead of seeking the most efficient algorithm, based on the principle of indifference [Keynes, 1921], the commonly used uniform distribution is assumed for the transition kernel  $q(y|x)$  ( $y \sim U[x - \Delta x, x + \Delta x]$ ). And the uniform distributions is also assumed for the prior distribution  $P(\Theta)$  ( $\Theta \sim U[\Theta_{min}, \Theta_{max}]$ ) to further simplify the computation. Sampling is done independently for each parameter dimension as we assume no correlation between parameters here. The acceptance rate can then be computed by

$$\alpha_{x,y} = \frac{P(D|y)}{P(D|x)} \cdot \mathbf{1}_{[\Theta_{min}, \Theta_{max}]}(y) \quad (5)$$

where  $\mathbf{1}_A(y)$  is an indicator function which returns 1 if  $y \in A$  and 0 if not. Compared to the posterior distribution  $P(\Theta|D)$ , the likelihood distribution  $P(D|\Theta)$  is usually much easier to estimate when the governing model is already known. However, the simulated Markov process can be trapped by local optima when using the uniform transition kernel with small step sizes (i.e.  $\Delta x$ ) [Tjelmeland and Hegstad, 2001], and this effect is particularly significant when simulating high dimensional random variables. We propose to initialize the Markov process with a searching procedure

over some coarse grids in the range of  $[\Theta_{min}, \Theta_{max}]$ . The size of a coarse grid is set to  $\frac{\Theta_{max}-\Theta_{min}}{10}$  and thus the total number of grids is  $10^p$  for a  $p$ -dimensional parameter vector.  $P(D|\Theta)$  is estimated using parameter values of the middle point for each coarse grid and the parameter value that maximizes  $P(D|\Theta)$  is used to initiate the Markov chain. Performance and reasoning of this extra procedure are further evaluated in Section 4.1. In the following analysis, expectations of the simulated parameter samples are denoted by the Bayesian (optimal) parameter estimations.

### 3.2 The Instantaneous Unit Hydrograph Model

The Instantaneous Unit Hydrograph (IUH) model is a widely used conceptual model for runoff estimation and has a long history of successful implementation in hydrology [Gupta et al., 1980, Jakeman et al., 1990, Lee and Yen, 1997, Grimaldi et al., 2012]. And it is well-established that IUHs can reflect some physical properties of a watershed like geomorphology characteristics [Gupta et al., 1980, Lee and Yen, 1997, da Ros and Borga, 1997]. This fact suggests potential of monitoring changes in local hydrological response by tracking changes in IUHs. To study dynamics of IUHs in a quantitative way, here we propose to use a parameterized form as given by

$$h(t; \lambda, k, \theta) = \lambda \frac{1}{\Gamma(k)\theta^k} t^{k-1} e^{-t/\theta} \quad (6)$$

The formula is essentially a modified Gamma distribution:  $\lambda$  is a scaling factor that accounts for loss of water in runoff generation processes (e.g. evapotranspiration);  $(k, \theta)$  are shaping parameters for the Gamma distribution. The Gamma distribution is used for its flexibility in modeling different types of IUHs [Kirchner et al., 2000, Bhunya et al., 2003]. A time-invariant additive Gaussian noise ( $\varepsilon_t \sim N(0, \sigma^2)$ ) is assumed and the observed runoff can be approximated by

$$R(t) = \tilde{R}(t) + \varepsilon_t = \sum_0^T P(t-\tau)h(\tau; \lambda, k, \theta) + \varepsilon_t \quad (7)$$

where the resulting runoff  $\tilde{R}$  is modeled as convolution of precipitation and an IUH ( $\tilde{R}(t) = P(t) \otimes h(t; \Theta)$ ). Probability of runoff observations conditioned on a set of parameters  $(\lambda, k, \theta)$  can then be easily modeled using a Gaussian distribution  $R(t) \sim N(\tilde{R}(t), \sigma^2)$  and the acceptance rate in Equation 5 can be computed by

$$\alpha_{x,y} = \exp \left( \frac{-1}{2\sigma^2} \sum_{t=1}^N (R(t) - \tilde{R}(t; h(y)))^2 - \frac{-1}{2\sigma^2} \sum_{t=1}^N (R(t) - \tilde{R}(t; h(x)))^2 \right) \cdot \mathbf{1}_{[\Theta_{min}, \Theta_{max}]}(y) \quad (8)$$

For situations where the noise level is known (Section 4.1),  $\sigma^2$  can be predetermined. And for situations where the noise level is unknown (Section 4.2),  $\sigma^2$  can be approximated by the mean squared error (MSE) using the MLE parameter estimations [Stedinger et al., 2008] as given by

$$\sigma^2 = \frac{\sum_{t=1}^N (R(t) - \tilde{R}^{MLE}(t))^2}{N} \quad (9)$$

The physical interpretation of Equation 9 is that if we assume observations are governed by the proposed model, then MSE is minimized with the MLE parameters and should represent the true noise level. We replaced the MLE parameter estimations with the Bayesian parameter estimations and Equation 9 is implemented in an iterative way:

1. The PDF of  $P(\Theta|D)$  is simulated using MCMC with some arbitrarily assigned constant for  $\sigma^2$ .
2.  $R^{MLE}(t)$  is approximated using the Bayesian parameter estimations,
3.  $\sigma^2$  in step 1 is updated using Equation 9 and step 2-3 are repeated.

For simplicity, only one iteration is done in Section 4.2 and a prelim analysis showed that one iteration can already guarantee convergence for the approximated MLE  $\sigma^2$  ( $R^2 = 0.998$  for 65 samples comparing the approximated  $\sigma^2$ 's after one and two iterations).

Table 1: Ranges for parameter values  $[\Theta_{min}, \Theta_{max}]$ 

Parameters	$\lambda$	$k$	$\theta$
Ranges (simulation)	$[0, 0.8]$	$[0, 15]$	$[0, 0.8]$
Ranges (case study)	$[0, 0.6]$	$[0, 6]$	$[0, 10]$

## 4 Results & Discussions

### 4.1 A Simulation Analysis

The model is first tested with simulated precipitation and runoff data. The simulation length is set to one year (i.e. 52 weeks) and we assume parameters determining the IUH follow a seasonal cycle as described by a sinusoidal curve. For  $i^{th}$  week, the parameters are defined by

$$\lambda(i) = 0.6 - 0.1 \cdot (1 - \cos(\frac{2\pi}{52} \cdot i)) \quad (10)$$

$$k(i) = 10 - 4.5 \cdot (1 - \cos(\frac{2\pi}{52} \cdot i)) \quad (11)$$

$$\theta(i) = 0.2 + 0.2 \cdot (1 - \cos(\frac{2\pi}{52} \cdot i)) \quad (12)$$

Seasonality of precipitation-runoff response is modeled by making evapotranspiration stronger (i.e. more loss of water and smaller  $\lambda$ ) and water travel time shorter during summer. Also, we assume data is collected for one storm event per week with precipitation falling at the starting day and there is no carryover flow across weeks. For each week, precipitation intensity at the starting day is determined by sampling from an uniform distribution ( $P(i) \sim U[1, 2]$ ). Noisy runoff observations are generated by adding a time-invariant Gaussian noise ( $\varepsilon \sim N(0, \sigma^2 = 0.002^2)$ ) to convolution of precipitation and the IUH ( $R(t) = P(t) \otimes h(t; \lambda(i), k(i), \theta(i)) + \varepsilon$ ). The unit for  $P(i)$  and  $\varepsilon$  is [10mm] and the simulated precipitation and runoff are plotted in Figure 1. Parameter value ranges for the prior distributions  $[\Theta_{min}, \Theta_{max}]$  are listed in Table 1.  $T$  is set to 7 days, and step size  $\Delta x$  in the transition kernel is set to (0.005, 0.05, 0.005) for  $(\lambda, k, \theta)$ .

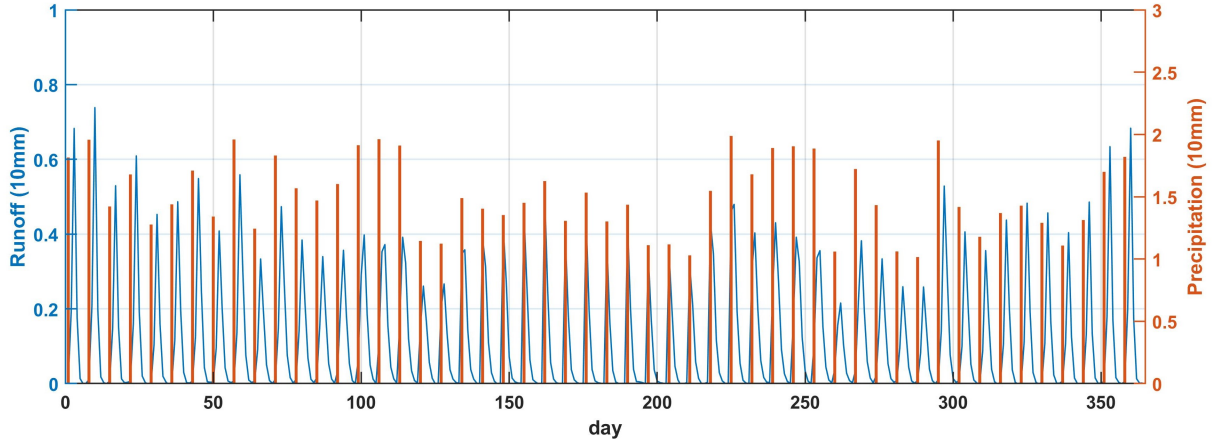


Figure 1: The simulated precipitation (red bar) and runoff (blue line)

Performance of the extra layer of searching optimal initial parameter values over coarse grids is examined using the simulated data of precipitation and runoff. Mean relative errors are computed and compared for Bayesian parameter estimations initiated with random values and with the searching procedure as shown in Figure 2. For each case of initialization, the experiment was repeated for 50 random seeds to further study convergence of the initial searching procedure. Significantly greater errors as well as uncertainty ranges are observed for models initiated with random parameter values. By initiating the model with an extra searching procedure over coarse grids, expectation performance

and robustness are markedly improved as the upper limits of relative errors dropped to below 2.5% for all parameters across 50 random seeds.

By further comparing parameter estimations against true values as shown in Figure 3, we found that the poor performance with random initial values can be resulted from the combined effects of local extremum 'traps' and small step size of the transition kernel. With the simplifications, the model essentially aggregates deviance between  $\tilde{R}(t; h(y))$  and the observed  $R(t)$  into a one-dimensional metric in computing  $\alpha_{x,y}$  and therefore, the multi-dimensional information can be lost and there can be some local extrema with incorrect combinations of parameter values. And since we are using a rather small step size for the transition kernel, the searching can be trapped by these local extrema. For estimations initiated with random values, on average only around 60% of the 52 samples (weeks) converge to the true value (or the global optimum). And the convergence ratio is 98% for estimations initiated with the extra searching procedure. We then compared relative errors of model estimations that converge to the true value and found very negligible difference (less than 5%) for the two cases using different ways of initialization across all three parameters. The results suggest that difference in model skill observed in Figure 2 is solely caused by difference in convergence ratios.

We further looked into the convergence problem by separately studying effects of parameters from two groups: 1) the scaling parameter  $\lambda$  and 2) the shape parameters  $(k, \theta)$ . For  $\lambda$ , if we fix  $(k, \theta)$ , it is easy to figure that  $P(D|\lambda)$  is a convex function of  $\lambda$  by analytically solving for the first and second derivatives of  $\log(P(D|\lambda))$  to  $\lambda$ . This indicates that  $\lambda$  would not cause any convergence problem in minimizing  $P(D|\lambda)$  since the function does not have multiple local minima. For  $(k, \theta)$ , since analytical solutions for the first and second derivatives are much harder and more complicated to derive, we numerically computed and mapped runoff MSE in the parameter space (since the runoff MSE has a monotonic inverse relationship with  $P(D|k, \theta)$ ). The response surface is featured with two 'valleys' separated by a steep 'ridge': the two 'valleys' represent two local minima of runoff MSE and the 'ridge' represents areas with high MSE (as seen in Figure S1). Since we used rather tiny step sizes for the transitional kernel, the Markov chain cannot escape from one 'valley' when initiated with improper values, and this would lead to the convergence problem. Also, the results suggest  $(k, \theta)$  would always converge to the true values at the same time because they are correlated in the response surface. Further details can be seen in the section of Supplementary Material.

Our analysis proved validity of the initial searching procedure since it guarantees that Markov chain will almost always be initiated in the right 'valley'  $\circ$ . However, it should be noted that this procedure is not the smartest solution since the computational cost still increases exponentially as dimensionality of the parameter space increases. The convergence problem can be solved with other methods like a restarting algorithm and using adaptive transition kernels (there are many advanced techniques in choosing and implementing efficient and adaptive transition kernels [Brockwell and Kadane, 2005, Andrieu and Moulines, 2006, Roberts and Rosenthal, 2009]). But our intent is to examine feasibility of the whole Bayesian framework in estimating hydrology model parameters and thus we only adopt this initial searching procedure for simplicity.

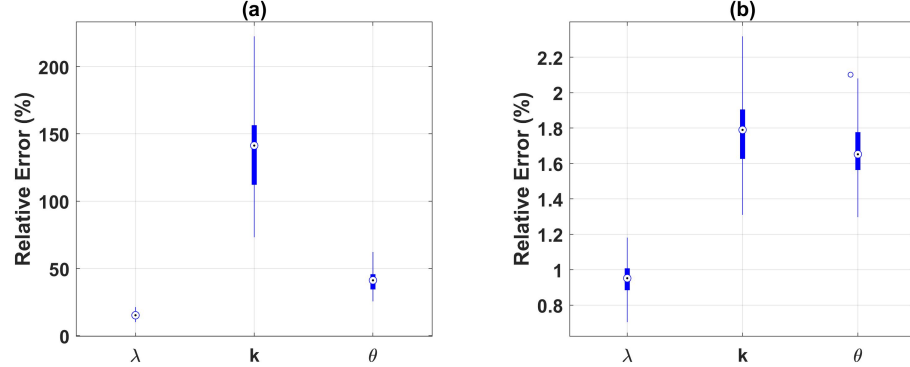


Figure 2: Box plots of relative errors in parameter estimations with random initial values (a) and with initial searching over coarse grids (b).

#### 4.2 A Case Study for the Fall Creek Watershed

The model is then tested using observational data of precipitation and runoff collected from the Fall Creek watershed. Unlike the simulation experiment, parameter values are estimated using data over the whole summer period (of which the length varies from 92 to 97 days) for each year. Further detailed description of data can be seen in Section 2. Since

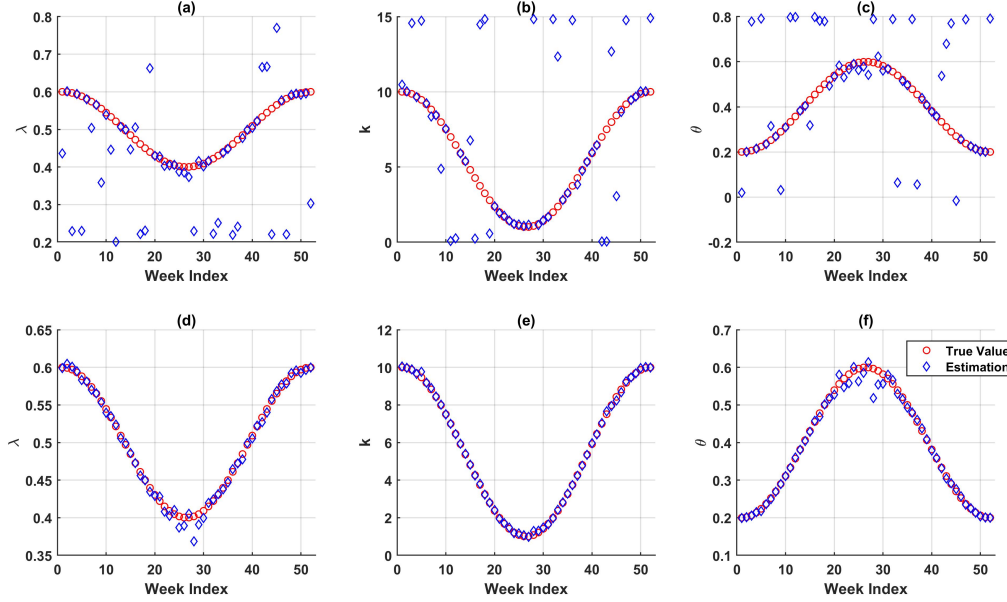


Figure 3: Comparison between the estimated (blue diamond) and true (red circle) parameter values with random initial values (a, b, c) and with initial searching over coarse grids (d, e, f) for  $\lambda$  (a, d),  $k$  (b, e), and  $\theta$  (c, f) for one random seed.

true parameter values are unknown for the case study, the MLE estimations are computed by randomly searching in the parameter space  $[\Theta_{min}, \Theta_{max}]$  to minimize MSE between the observed and estimated runoff. The MLE parameter estimations represent the best possible parameter values given the Gamma distribution-based IUH formula we are using in this study. Rather broad ranges are assigned for the parameter space and the same ranges are used to determine the prior distributions for the Bayesian model as listed in Table 1.  $T$  is set to 14 days, which should be long enough to model the lasting effects of most storm events for the Fall Creek watershed. Step size  $\Delta x$  of transitional kernel is set to  $(0.005, 0.05, 0.1)$  for  $(\lambda, k, \theta)$ .

We first compared model skill of the IUH-based runoff estimations (against runoff observations) using the MLE parameter estimations and the Bayesian parameter estimations as shown in Figure 4. Comparably good model skill is observed for runoff estimations using both set of parameters: the median CCs are greater than 0.7 and the median NSE scores are greater than 0.49 for both sets of parameter estimations. The results of good model skill should also validate the Gamma distribution-based IUH in estimating runoff for the Fall Creek watershed. No statistical significance levels are plotted here because the effective degrees of freedom heavily depend on autocorrelations in the data [Afyouni et al., 2019] and vary significantly across years (since autocorrelations in runoff/precipitation are largely affected by frequencies and intensities of storm events).

The Bayesian parameter estimations are then compared against their MLE counterparts as shown in Figure 5. Great consistency is observed between the MLE and Bayesian parameter estimations: the  $R^2$  values are 0.95, 0.62, and 0.64 for  $(\lambda, k, \theta)$  as calculated based on the 1 : 1 reference line. Of the three parameters, the highest  $R^2$  value is found for  $\lambda$ . A possible explanation can be that the IUH is more 'sensitive' to  $\lambda$  since it solely determines integral (i.e. amplitude) of the IUH while the two other parameters ( $k, \theta$ ) only collectively determine shape of the IUH. Different combinations of  $(k, \theta)$  can result in very similar IUH shapes and therefore, more deviations between the MLE and Bayesian estimations are understandable for  $(k, \theta)$ .

Also, the Bayesian estimations of  $\lambda$  are found to be consistent with the runoff coefficients computed by dividing the total amount of runoff by the total amount of precipitation for each summer period. The  $R^2$  value calculated based on the 1 : 1 reference line is 0.65 and the correlation coefficient is 0.87 for 65 samples (one-tailed p-value  $< 0.001$ ). On one hand, this should further prove validity of the Gamma distribution-based IUH in modeling local precipitation-runoff response since the parameter  $\lambda$  is a scaling coefficient designed to account for the actual loss of water. On the other hand, the runoff coefficients can be regarded as the true  $\lambda$  values and the results show that the Bayesian model achieved great performance in estimating the time-varying hidden variables.

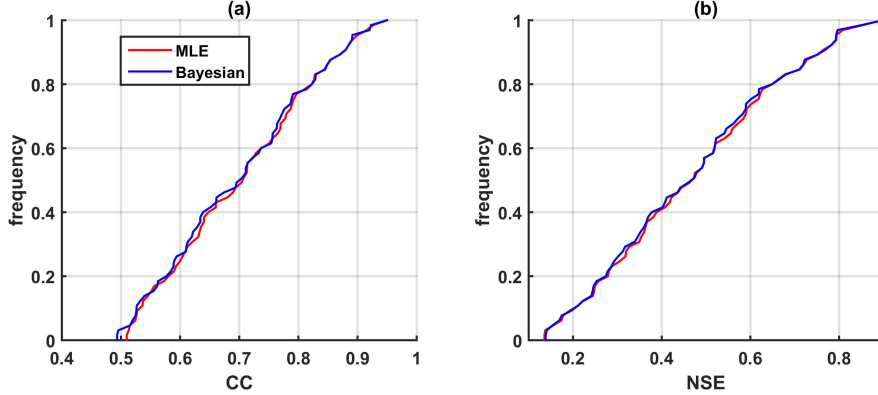


Figure 4: Empirical cumulative distribution functions for model skill of runoff estimations as measured by Pearson's correlation coefficients (CC) and Nash-Sutcliffe Efficiency (NSE) scores. Model skill using MLE estimations and Bayesian estimations are plotted in blue and red curves.

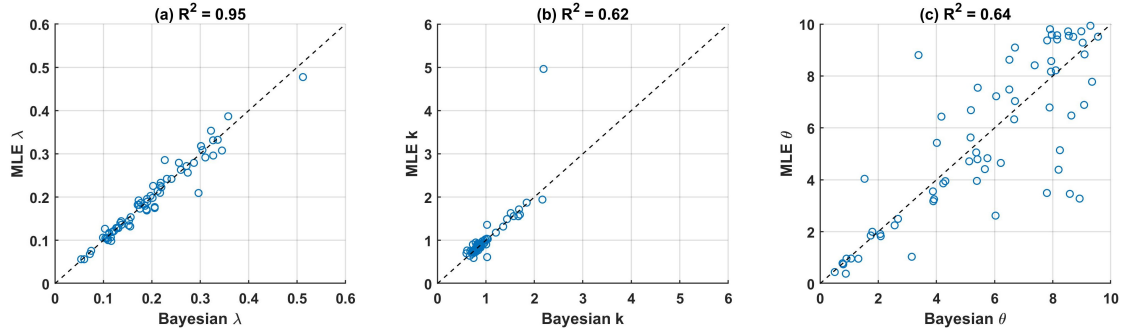


Figure 5: Comparison between the Bayesian (x axis) and MLE (y axis) parameter estimations for (a)  $\lambda$ , (b)  $k$ , and (c)  $\theta$ . The 1 : 1 reference lines are plotted in black dashed lines.

At last, we studied dynamics of the local precipitation-runoff responses by looking at the IUHs through the whole study period of 1925-2017. Since it is hard to compare IUHs of different shapes in a quantitative way, we first define two types of IUHs that have distinctly different physical interpretations. The IUHs that monotonically decreases over time are defined as the 'diffusion' type while those with wave-like distributions are defined as the 'advection' type. A schematic of the two IUH types is shown in Figure 6. The two types can have direct use in informing flooding mitigation since they determine the timing and rate of peak flow differently. Also, the two IUH types can reflect different water travel times, and therefore indicate different hydrological properties.

Time series of IUH types as well as rescaled runoff coefficients, precipitation and runoff are plotted in Figure 7. The 'advection' IUHs are given values of 1 and the 'diffusion' IUHs are given values of 0. The runoff coefficients, precipitation and runoff are linearly normalized to the range of [0, 1]. Interestingly, a systematic shift is observed for the IUH type: before 1942-1943, the local IUH is dominated by the 'advection' type; after 1942-1943, the local IUH switched to the 'diffusion' type. However, this change cannot be detected from the easy-to-measure variables including summer precipitation, runoff and runoff coefficients since no significant change in amplitude is observed around 1942-1943 for these variables. This suggests that the change could occur only in the temporal distribution of runoff generation. Physically, the systematic change can indicate that water in the Fall Creek watershed flows faster (i.e. has shorter travel time) after 1942-1943, which can possibly be caused by change of land uses (e.g. construction of paved roads). However, we could not find any support evidence from historic records of the Fall Creek watershed and Ithaca water & sewer systems. Interestingly, the systematic change coincided with relocation of the precipitation stations when Cornell moved its precipitation stations from the Roberts Hall (on ground outside of the building) [42°26'55"N, 76°28'45"W] to the College of Agriculture Experimental Farm at Caldwell Field in June 1943 [42°26'56"N, 76°27'38"W]. While the relocation of station can lead to change in latency between precipitation and runoff observations, we expect the effects to be minor since 1) the precipitation station was only move one mile east in 1943 (for reference a hurricane typically moves at a forward speed of 5-20 miles per hour [King and Shemdin, 1978]), and 2) the precipitation station was moved again to its current location on Game Farm Road [42°26'57"N, 76°26'57"W] in June 1969 but we did not observe any

changes in IUHs. But still, the Bayesian model managed to detect a systematic shift in the local precipitation-runoff response that cannot be learned by looking at the easy-to-measure variables.

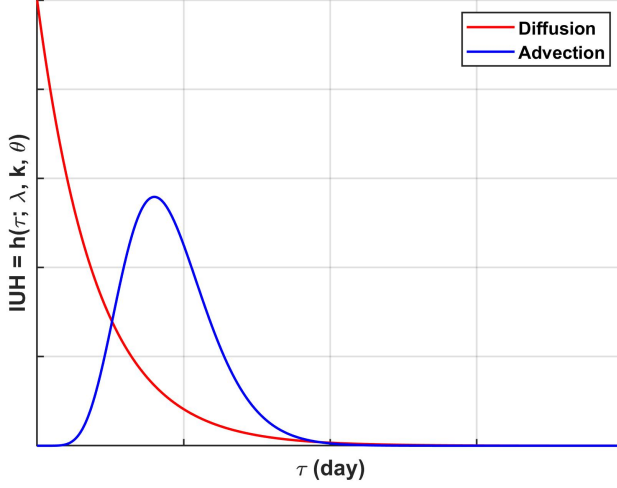


Figure 6: A schematic of the two types of IUHs: the 'diffusion' type (red) and the 'advection' type (blue).

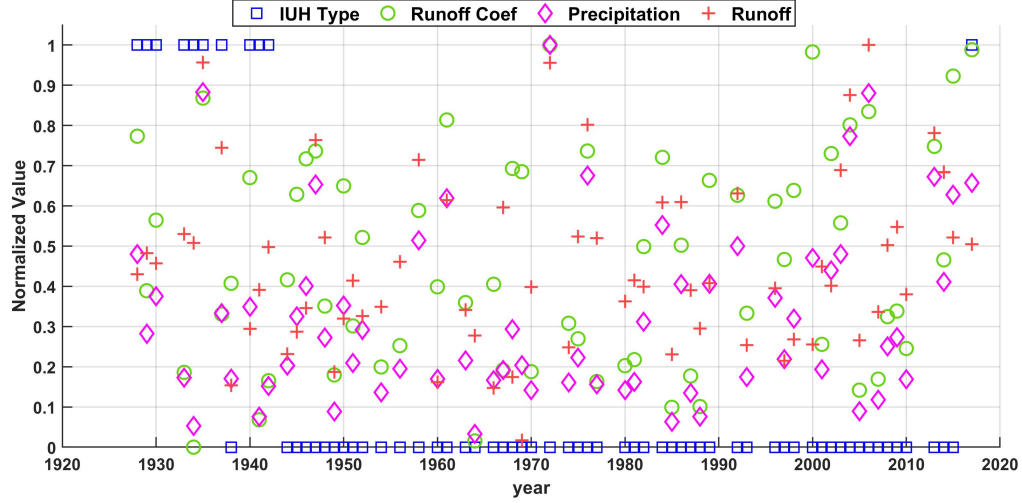


Figure 7: Time series of normalized values (in the range of  $[0, 1]$ ) for IUH types (blue squares), runoff coefficients (green circles), precipitation (purple diamonds), and runoff (red crosses). The 'advection' IUHs are given values of 1 while the 'diffusion' IUHs are given values of 0.

## 5 Conclusion

In this study, we examined performance of a Bayesian inference model (i.e. MCMC) in estimating hydrology model parameters given observations of precipitation and runoff for small watersheds. The IUH conceptual model based on a modified Gamma distribution was adopted and the whole framework was tested using both simulated and observational data. In the simulation analysis, we investigated the convergence problem in MCMC and found that the simulated Markov chain could be trapped by some local optima in the parameter space of  $(k, \theta)$ . An extra procedure of searching over coarse parameter grids in choosing initial values can significantly reduce errors in parameter estimations by avoiding the convergence problem and was added to the framework. In the case study, the framework was tested using observational data of precipitation and runoff over 1925-2017. Since true values were not known, the MLE parameter

estimations were used as the best possible parameter values. Comparable model skill was observed for the MLE and Bayesian runoff estimations and great consistency was observed between the MLE and Bayesian parameter estimations. A systematic shift was identified in the IUH patterns which suggested a possibly shorter travel time for water after 1943 and the shift could not be learned by looking at the easy-to-measure variables like precipitation, runoff, and runoff coefficients. The underlying cause remains unknown since the shift could be resulted from changes of local land use types (e.g. construction of paved roads) or relocation of the precipitation station. Overall, our study demonstrated feasibility of the Bayesian framework in monitoring hydrological dynamics and detecting change points for small watersheds by tracking the hidden variables (i.e. model parameters). The model can further be used to adaptively modify local strategies in water resource management and disaster mitigation since it can rapidly reflect changes in local precipitation-runoff response by using updated observational data.

## 6 Acknowledgement

We want to thank Dr. Wilfried Brutsaert from the School of Civil and Environmental Engineering at Cornell for his helpful comments on historical hydrology conditions of the Fall Creek watershed, William Coon from USGS for compiling historic record of the runoff gauge, and Keith Eggleston and Mark Wysocki from the Department of Earth and Atmospheric Sciences at Cornell for compiling historic record of the precipitation station.

## 7 Supplementary Material

The IUH parameters are divided into two groups and their effects are examined separately here. First, we fix  $(k, \theta)$  and only alter the scaling parameter  $\lambda$ .  $P(D|\lambda)$  can then be computed as given by

$$\log(P(D|\lambda)) = \text{const} \cdot \sum_{i=1}^n (R(i) - P(i) \otimes h(i; \lambda))^2 = \text{const} \cdot \sum_{i=1}^n (R(i) - \lambda \cdot K(i))^2 \quad (13)$$

where  $K(t) = P(t) \otimes h(t)/\lambda$  and  $K(i) > 0, \forall i$ . If we drop the constant term, the derivative is given by

$$\frac{\partial \log(P(D|\lambda))}{\partial \lambda} = \sum_{i=1}^n (2K(i)^2 \lambda - 2R(i)K(i)) = \lambda \sum_{i=1}^n 2K(i)^2 - \sum_{i=1}^n 2R(i)K(i) \quad (14)$$

$\log(P(D|\lambda))$  and thus  $P(D|\lambda)$  are convex functions of  $\lambda$  (with fixed  $(k, \theta)$ ). The minimum is only reached at  $\lambda = \frac{\sum_{i=1}^n R(i)K(i)}{\sum_{i=1}^n K(i)^2}$  or one of the end points. Therefore, the traps of multiple local minima do not exist for  $\lambda$  and we do not have to worry about convergence of MCMC with varying  $\lambda$ s.

However, to analytically solve for derivatives of  $P(D|k, \theta)$  to  $(k, \theta)$  is hard. For the shape parameters, we numerically computed runoff MSE ( $MSE = \sum_{i=1}^n (R(i) - P(i; k, \theta))^2$ ) as a function of  $(k, \theta)$ . Since  $\log(P(D|k, \theta))$  is proportional to the MSE, we can instead examine the response surface of MSE to imply the convergence condition of  $\log(P(D|k, \theta))$ . The response surface averaged for all  $\lambda$ s is plotted in Figure S1. The MSE map is divided into two 'valleys' (low MSE and high  $P(D|k, \theta)$ ) by a 'ridge' (high MSE and low  $P(D|k, \theta)$ ). The simulated Markov chain tends to move downslope to one of the 'valleys' and when initiated with impropoer values, it could get stuck in the wrong 'valley' (a local but not global minimum). After examining the MSE response surfaces for all  $\lambda$  values, we found the two 'valley' pattern was pretty consistent and some snapshots are shown in Figure S2. This should also explains why the effect of the scaling parameter  $\lambda$  is relatively independent from that of the shape parameters  $(k, \theta)$ :  $(k, \theta)$  are correlated and always converge to the global optimum at the same time while the convergence is not affected by changing values of  $\lambda$ .

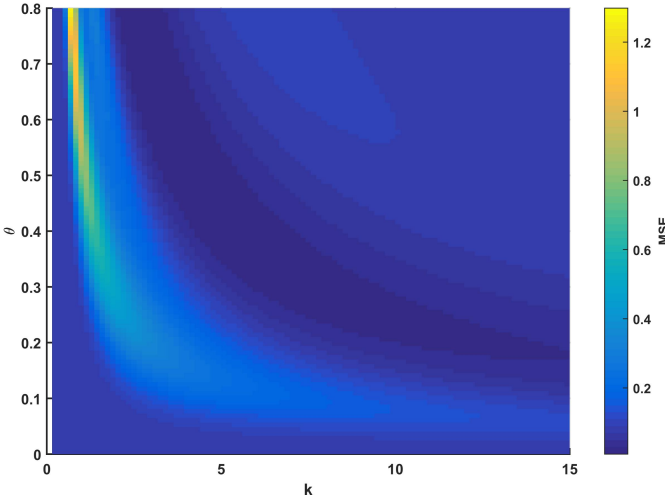


Figure 8: The response surface of runoff MSE as function of  $(k, \theta)$  averaged for all  $\lambda$ s

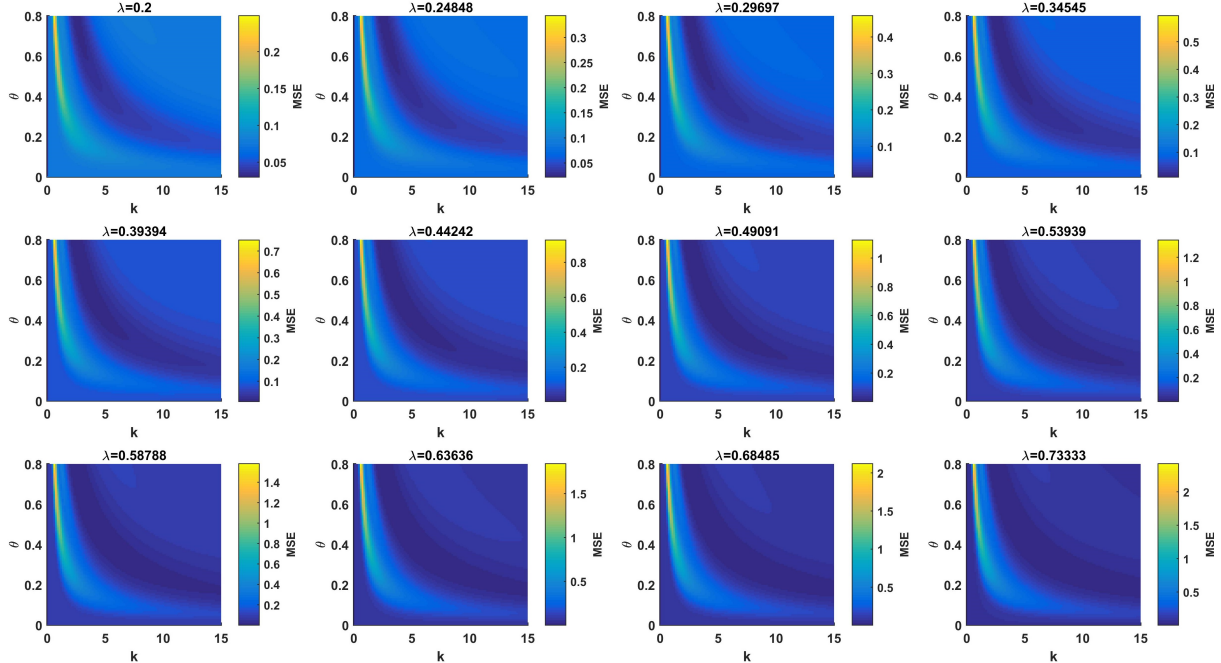


Figure 9: The response surfaces of runoff MSE as function of  $(k, \theta)$  for varying  $\lambda$  values

## References

Zhiqiang Jiang, Rongbo Li, Anqiang Li, and Changming Ji. Runoff forecast uncertainty considered load adjustment model of cascade hydropower stations and its application. *Energy*, 158:693–708, 2018.

Reepal Shah, Atul Kumar Sahai, and Vimal Mishra. Short to sub-seasonal hydrologic forecast to manage water and agricultural resources in india. *Hydrology and Earth System Sciences*, 21(2):707–720, 2017.

Florian Pappenberger, Keith J Beven, NM Hunter, PD Bates, Bingo T Gouweleeuw, J Thielen, and APJ De Roo. Cascading model uncertainty from medium range weather forecasts (10 days) through a rainfall-runoff model to flood inundation predictions within the european flood forecasting system (effs). *Hydrology and Earth System Sciences*, 9(4):381–393, 2005.

Felix Fundel, Stefanie Jörg-Hess, and Massimiliano Zappa. Monthly hydrometeorological ensemble prediction of streamflow droughts and corresponding drought indices. *Hydrology and Earth System Sciences*, 17(1):395–407, 2013.

Juraj M Cunderlik and Taha BMJ Ouarda. Trends in the timing and magnitude of floods in canada. *Journal of hydrology*, 375(3-4):471–480, 2009.

Hong Xuan Do, Fang Zhao, Seth Westra, Michael Leonard, Lukas Gudmundsson, Julien Eric Stanislas Boulange, Jinfeng Chang, Philippe Ciais, Dieter Gerten, Simon N Gosling, et al. Historical and future changes in global flood magnitude—evidence from a model–observation investigation. *Hydrology and Earth System Sciences*, 24(3):1543–1564, 2020.

Yan Ma, Haiping Wu, Lizhe Wang, Bormin Huang, Rajiv Ranjan, Albert Zomaya, and Wei Jie. Remote sensing big data computing: Challenges and opportunities. *Future Generation Computer Systems*, 51:47–60, 2015.

Marwan A Hassan, Roey Egozi, and Gary Parker. Experiments on the effect of hydrograph characteristics on vertical grain sorting in gravel bed rivers. *Water Resources Research*, 42(9), 2006.

Griet Heuvelmans, Bart Muys, and Jan Feyen. Evaluation of hydrological model parameter transferability for simulating the impact of land use on catchment hydrology. *Physics and Chemistry of the Earth, Parts A/B/C*, 29(11-12):739–747, 2004.

Soroosh Sorooshian, Vijai Kumar Gupta, and James Lloyd Fulton. Evaluation of maximum likelihood parameter estimation techniques for conceptual rainfall-runoff models: Influence of calibration data variability and length on model credibility. *Water Resources Research*, 19(1):251–259, 1983.

Simone Castiglioni, Laura Lombardi, Elena Toth, Attilio Castellarin, and Alberto Montanari. Calibration of rainfall-runoff models in ungauged basins: A regional maximum likelihood approach. *Advances in Water Resources*, 33(10):1235–1242, 2010.

Bryson C Bates and Edward P Campbell. A markov chain monte carlo scheme for parameter estimation and inference in conceptual rainfall-runoff modeling. *Water resources research*, 37(4):937–947, 2001.

Tyler Jon Smith and Lucy Amanda Marshall. Bayesian methods in hydrologic modeling: A study of recent advancements in markov chain monte carlo techniques. *Water Resources Research*, 44(12), 2008.

Samuel P Nolan, Luca Pezzè, and Augusto Smerzi. Frequentist parameter estimation with supervised learning. *arXiv preprint arXiv:2105.12302*, 2021.

Devinderjit Sivia and John Skilling. *Data analysis: a Bayesian tutorial*. OUP Oxford, 2006.

Mary Kathryn Cowles and Bradley P Carlin. Markov chain monte carlo convergence diagnostics: a comparative review. *Journal of the American Statistical Association*, 91(434):883–904, 1996.

Bin Ba, Weijia Cui, Daming Wang, and Jianhui Wang. Maximum likelihood time delay estimation based on monte carlo importance sampling in multipath environment. *International Journal of Antennas and Propagation*, 2017, 2017.

Gayathri K Devia, B Pa Ganasri, and G Sa Dwarakish. A review on hydrological models. *Aquatic procedia*, 4:1001–1007, 2015.

James O Knighton, Arthur DeGaetano, and M Todd Walter. Hydrologic state influence on riverine flood discharge for a small temperate watershed (fall creek, united states): negative feedbacks on the effects of climate change. *Journal of Hydrometeorology*, 18(2):431–449, 2017.

Zachary M Easton, Pierre Gérard-Marchant, M Todd Walter, A Martin Petrovic, and Tammo S Steenhuis. Hydrologic assessment of an urban variable source watershed in the northeast united states. *Water Resources Research*, 43(3), 2007.

Helen E Dahlke, Zachary M Easton, Daniel R Fuka, Steve W Lyon, and Tammo S Steenhuis. Modelling variable source area dynamics in a ceap watershed. *Ecohydrology: Ecosystems, Land and Water Process Interactions, Ecohydrogeomorphology*, 2(3):337–349, 2009.

U.S. Geological Survey. Usgs water data for the nation, 1994. URL <https://waterdata.usgs.gov/nwis>.

Imke Durre, Matthew J Menne, and Russell S Vose. Strategies for evaluating quality assurance procedures. *Journal of Applied Meteorology and Climatology*, 47(6):1785–1791, 2008.

Imke Durre, Matthew J Menne, Byron E Gleason, Tamara G Houston, and Russell S Vose. Comprehensive automated quality assurance of daily surface observations. *Journal of Applied Meteorology and Climatology*, 49(8):1615–1633, 2010.

Matthew J Menne, Imke Durre, Russell S Vose, Byron E Gleason, and Tamara G Houston. An overview of the global historical climatology network-daily database. *Journal of atmospheric and oceanic technology*, 29(7):897–910, 2012.

Greg Welch, Gary Bishop, et al. An introduction to the kalman filter. 1995.

Sean R Eddy. What is a hidden markov model? *Nature biotechnology*, 22(10):1315–1316, 2004.

Walter R Gilks, Sylvia Richardson, and David Spiegelhalter. *Markov chain Monte Carlo in practice*. CRC press, 1995.

Siddhartha Chib and Edward Greenberg. Understanding the metropolis-hastings algorithm. *The american statistician*, 49(4):327–335, 1995.

Ziheng Yang and Carlos E Rodríguez. Searching for efficient markov chain monte carlo proposal kernels. *Proceedings of the National Academy of Sciences*, 110(48):19307–19312, 2013.

Yuttapong Thawornwattana, Daniel Dalquen, and Ziheng Yang. Designing simple and efficient markov chain monte carlo proposal kernels. *Bayesian Analysis*, 13(4):1037–1063, 2018.

John Maynard Keynes. Chapter iv: The principle of indifference. volume 4, pages 41–64. Macmillan and Company, limited, 1921.

Hakon Tjelmeland and Bjorn Kare Hegstad. Mode jumping proposals in mcmc. *Scandinavian journal of statistics*, 28(1):205–223, 2001.

Vijay K Gupta, Ed Waymire, and CT Wang. A representation of an instantaneous unit hydrograph from geomorphology. *Water resources research*, 16(5):855–862, 1980.

AJ Jakeman, IG Littlewood, and PG Whitehead. Computation of the instantaneous unit hydrograph and identifiable component flows with application to two small upland catchments. *Journal of hydrology*, 117(1-4):275–300, 1990.

Kwan Tun Lee and Ben Chie Yen. Geomorphology and kinematic-wave–based hydrograph derivation. *Journal of Hydraulic Engineering*, 123(1):73–80, 1997.

S Grimaldi, A Petroselli, and F Nardi. A parsimonious geomorphological unit hydrograph for rainfall–runoff modelling in small ungauged basins. *Hydrological Sciences Journal*, 57(1):73–83, 2012.

Diego da Ros and Marco Borga. Use of digital elevation model data for the derivation of the geomorphological instantaneous unit hydrograph. *Hydrological processes*, 11(1):13–33, 1997.

James W Kirchner, Xiaohong Feng, and Colin Neal. Fractal stream chemistry and its implications for contaminant transport in catchments. *Nature*, 403(6769):524–527, 2000.

PK Bhunya, SK Mishra, and Ronny Berndtsson. Simplified two-parameter gamma distribution for derivation of synthetic unit hydrograph. *Journal of Hydrologic Engineering*, 8(4):226–230, 2003.

Jery R Stedinger, Richard M Vogel, Seung Uk Lee, and Rebecca Batchelder. Appraisal of the generalized likelihood uncertainty estimation (glue) method. *Water resources research*, 44(12), 2008.

Anthony E Brockwell and Joseph B Kadane. Identification of regeneration times in mcmc simulation, with application to adaptive schemes. *Journal of Computational and Graphical Statistics*, 14(2):436–458, 2005.

Christophe Andrieu and Éric Moulines. On the ergodicity properties of some adaptive mcmc algorithms. *The Annals of Applied Probability*, 16(3):1462–1505, 2006.

Gareth O Roberts and Jeffrey S Rosenthal. Examples of adaptive mcmc. *Journal of computational and graphical statistics*, 18(2):349–367, 2009.

Soroosh Afyouni, Stephen M Smith, and Thomas E Nichols. Effective degrees of freedom of the pearson’s correlation coefficient under autocorrelation. *NeuroImage*, 199:609–625, 2019.

DB King and OH Shemdin. Radar observation of hurricane wave directions. In *Coastal Engineering 1978*, pages 209–226. 1978.